1. Mykhaylo ZAGIRNYAK[1], 2. Oleksandr SALENKO[2], 3. Walid ALNUSIRAT[3], 4. Leonid GOLOVKO[2], 5. Vadym OREL[4], 6. Viktoriia KULYNYCH[1]

Kremenchuk Mykhailo Ostrohradskyi National University (1), Sikorskyi NTUU KPI (2), Al-Balqa Applied University (3), Kremenchuk flight college Kharkiv National University of Internal Affairs Kremenchuk (4)
ORCID: 1. 0000-0003-4700-0967, 2. 0000-0002-5685-6225, 3. 0000-0002-9604-3165, 4. 0000-0001-7803-0312, 5. 0000-0002-8775-3253, 6. 0000-0003-1702-2989

doi:10.15199/48.2024.03.52

Increasing the Strength of Thin-walled Products Obtained by FDM Using the Thin Surface Films

Abstract. *A review and analysis of methods for the obtaining the products with surface films. The possibility of increasing the strength of shell products under the action of thermobaric load and establishing the functional conditioning of the strength limit by the conditions of formation of protective films is presented.*

Streszczenie. *Przegląd i analiza metod otrzymywania wyrobów z foliami powierzchniowymi. Przedstawiono możliwość zwiększenia wytrzymałości wyrobów powłokowych pod wpływem obciążenia termobarycznego i ustalenia funkcjonalnego uwarunkowania granicy wytrzymałości warunkami tworzenia się filmów ochronnych.* ***(Zwiększanie wytrzymałości cienkościennych produktów uzyskanych metodą FDM przy użyciu cienkich folii powierzchniowych)***

Keywords: FDM, surface films, strength, surface layers.
Słowa kluczowe: FDM, folie powierzchniowe, wytrzymałość, warstwy powierzchniowe

Introduction

The problem of high-quality, fast and economical repair of mechatronic systems in conditions of limited production capabilities is mentioned in [1]. Damaged parts restoration in original copies leads to a significant increase in the cost and work duration, making such repairs ineffective [2].

For aircraft, the supporting elements need repair: centerplanes, engine skins, supporting planes, stabilizers, etc. Such products are parts of a complex profile with thin walls, as a result of which there are certain technological approaches to their manufacture.

The use of 3D printing tools often allows restoring damaged parts through reverse engineering [3]. Important factors influencing the process are: layer thickness, method of stacking layers, thermodiffusion processes, etc. [4]. Stiffness, hardness and Young's moduli are determined by the material [5], [6], printing conditions and features of the additive process [7].

The active development of composite materials on a polymer basis reveals significant prospects for additive means: the material can be formed by a preliminary mixture of powders [8], the composition of the filament [9], and in the process of extrusion or laying [10]. As a result, it is possible to increase the strength by 20-40%, also increasing the properties anisotropy, in particular the difference between E_x, E_y, E_z; σ_x σ_y σ_z, [11]. Another way to increase strength is to change the topology of filament laying, or the conditions for the formation of workpiece microvolumes [12]. Work is actively underway to create polymer printers with additional axes [13-15]. There are fairly simple solutions for axisymmetric shells, given in particular in [16]. Moving away from planar laying of the filament also allows you to increase the strength of printed products, in particular, by 15-30%, [17].

The most commonly used plastics include PLA, ABS, PC, etc. They differ in their properties, require slightly different conditions for teaching, but these plastics are low-temperature. This prevents the residual stresses occurrence, which lead to the development of interlayer adhesion, cohesive destruction and deformation of the product as a whole.

For engineering tasks, strong high-temperature plastics are used, in particular, REEK, Ultem and PPSF. Extrusion of these materials takes place at a temperature of 425 °C. REEK is a promising plastic for creating shell products, as the strength limit is 110 MPa.

Currently, several main directions can be singled out for increasing the strength of products obtained by FDM: 1) changing the filament composition [10], 2) establishing rational process conditions [11], which reduces the number of structural defects; 3) rational topology of filament laying [12], changing the extrusion conditions and direction; 4) additional protective layers and films formation [13].

So the topic of the current research is determining the possibility of increasing the strength of shell products under the action of thermobaric load and establishing the functional conditioning of the strength limit by the conditions of formation of protective films

Research materials

The analysis of defects formed simultaneously with the creation of the model is described in [14]. A number of factors contribute to the defects formation: the extrusion conditions and filament laying, the constancy of the laying conditions, and the peculiarities of supplying energy to the affected zone. The same factors can affect the surface film formation mentioned in [15]. Bringing energy to the zone of influence is an important factor that determines the energy intensity and efficiency of combining elementary volumes.

The use of a laser or an electron beam for sintering powder materials is a method of melting the layer and forming a reliable film. The method is used for selective laser melting (SLM), selective laser sintering (SLS) and electronic melting (EBM) [16]. Films can be formed from metals, ceramics and polymers [17].

Ultrasonic welding (UC), a solid-state method of welding metal seams, is widely used for metal lamination methods. Thanks to the low-temperature operation of the UC process, the production of metal multilayer FGM [18], metal matrix composites is possible.

Taking into account the fact that the films on the solid bodies surface, according to table 1, can be quite different both in terms of properties and in the application method, we will focus on the following application methods: "cold" - 1.1, 2.1. and "hot" - 4.2 (table 1).

This choice is due to the fact that for "hot" (4) film application methods, the laser (4.2) or electron beam (4.4) sintering method is the most appropriate; "cold" methods (2.1) and (2.3) involve electrochemical or vacuum deposition of a film on a conductive base.

"Cold" methods of surface films deposition (2.1-2.3,

Table 1), as well as the adhesives use (1.1, Table 1) do not cause problems and are developed [19].

Table 1 – Surface layers and their formation

	Continuous	Discrete	The formation principle
Surface film layers	1.Chemical		1.1. Chemical interaction with an additive
			1.2. Surface layer transformation
	2. Physical and technical		2.1. Deposition (vacuum)
			2.2. Diffusion
			2.3. Galvanic methods
	3.Mechanical		3.1. Charging
			3.2. Plastic deformation
	4. Thermophysical processes		4.1. Plasma
			4.2. Laser
			4.3. Arc

The creation of a Me film on the plastic sample surface has not been studied enough and is due to the fact that powerful energy flows concentrate on the surface layer and can cause melting or sublimation of the plastic base, destruction and deformation. On the other hand, the energy must be sufficient to ensure the fusion of Me particles, the formation of a sufficiently dense layer capable in carrying certain loads.

At the initial stage, the laser energy and the pulses duration were determined based on a number of conditions. The task was set in two versions: 1) metal particles are introduced into the surface layer of the product during filament laying by two extruders; 2) metal particles are injected through the laser emitter itself.

Consider the process of heating the body surface by a falling solid-state laser that creates local heating of the irradiation zone. At the same time, the absorbed energy density is determined using the equation [19]:

$$q(x) = q_0 \exp^{\left(-x^2/r^2\right)},$$

where q_0 – radiation power density in the center of the focusing spot; r – beam radius taking into account the radiation density distribution.

The heat conduction process in the volume of the workpiece material, which is limited by the region Ω, with the surface ∂Ω, can be described using: scalar temperature field: $T = T(P,t)$, vector heat flow field: $q = q(P,t)$, $P = \{(x,y,z)\} \in \Omega$, scalar field with specific thermal energy: $e = e(T)$. Boundary conditions on the outer surfaces at $\tau > 0$

$$\left\{\Gamma_1: \; -\lambda\frac{\partial t}{\partial n} = q_r; \Gamma_2: \quad \frac{\partial t}{\partial n} = 0; \Gamma_3: -\lambda\frac{\partial t}{\partial n} = \alpha(t - t_{\text{medium}}).\right.$$

Conditions at the contact boundary Γ_4 with $\tau > 0$:

$$\begin{cases} t\big|_{\partial_4^-} = t\big|_{\partial_4^+}, \\ -\lambda_- \dfrac{\partial}{\partial n}\Big|_{\partial_4^-} = \lambda_+ \dfrac{\partial T}{\partial}\Big|_{\partial_4^+} \end{cases}$$

$$\begin{cases} t < t_m - \dfrac{\Delta t}{2}, \lambda_1(t) = \lambda_s; \left[c_p(t)\rho(t)\right]_1 = c_{ps}\rho_s; \\ t_m - \dfrac{\Delta t}{2} \le t \le t_m + \dfrac{\Delta t}{2}, \lambda_1(t) = \lambda_s + \dfrac{\lambda_m - \lambda_s}{\Delta t} \\ \left(t - t_m + \dfrac{\Delta t}{2}\right); \\ \left[c_p(t)\rho(t)\right]_1 = c_{ps}\rho_s + \dfrac{c_{pm}\rho_m - c_{ps}\rho_s}{\Delta t}\left(t - t_m + \dfrac{\Delta t}{2}\right) + \\ + \dfrac{L_f}{\Delta t}; \\ t > t_m + \dfrac{\Delta t}{2}, \lambda_1(t) = \lambda_m; \left[c_p(t)\rho(t)\right]_1 = c_{pm}\rho_m; \end{cases}$$

where n – normal to the surface; q_r – power density; α – heat transfer coefficient; Γ_1 – irradiated surface, Γ_2 – surface of axial symmetry, Γ_3 – surfaces in contact with the external environment, Γ_4 – contact boundary of binder and matrix.

Calculation schemes for solving thermal problems are presented in fig. 1.

At the same time, taking into account the simultaneity with heating, there will be some transfer of energy deep into the workpiece, which is due to the thermal conductivity of its material.

The problem of the phase boundaries movement taking into account thermal conductivity in the assumption that heat spreads along the normal to the surface.

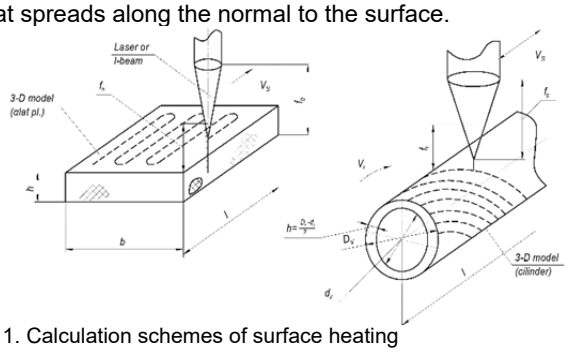

Fig 1. Calculation schemes of surface heating

For "cold" and "hot" film application, it is necessary to form a conductive surface layer. Conductive components such as finely dispersed graphite and copper particles were introduced into the model. These components were applied only in the outer layer of the model using a two-flow extruder, the parameters of which were determined through modeling in the Flow Simulation environment.

Modeling of the liquid movement in the channels of a two-flow extruder shows that even at movement speeds up to 120 mm/min, the melt movement remains laminar. There is practically no mixing of particles in the extruder channel. The particles move in a straight line relative to the axis of the channel after the opening of the particle supply channel. The delay time in movement (t_z) and the laying out accuracy (q) depend on the temperature in the extruder (T_e), the filament supply speed (v_f), particle mass and dimensions (m), fig. 2.

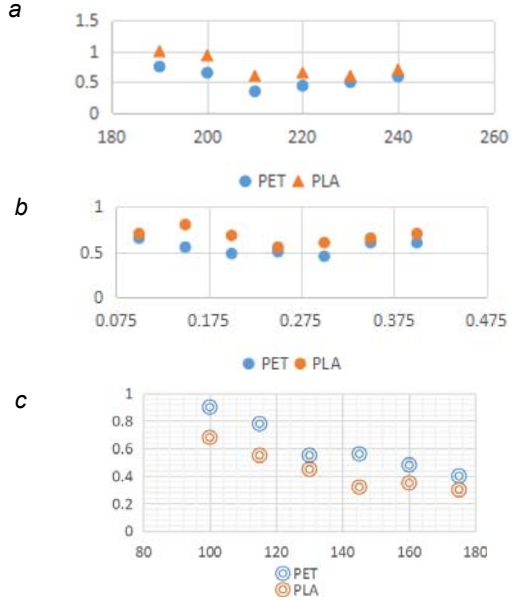

Fig 2. The influence of extrusion factors on the delay time t, sec, laying out parts on the plastic surface of the work table: a) temperature T, ^{0}C; b) particle size m, mm; c) teaching speed, v_f, mm/min

The absence of melt active mixing has a positive effect on predictions regarding the particles location on the surface. Examples of simulating the flow of liquids A and B in the extruder, as well as mixing, are shown in Fig. 3.

In order to increase the accuracy of modeling and predicting the product ultimate strength, the critical values of the test samples fracture stresses were estimated, and their correlation with the temperatures in the plastic deposition zone was established, fig. 4.

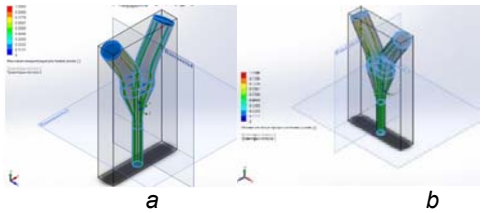

a *b*

Fig. 3. Interaction of two flows in the extruder (a) and mixing of the mixture at the outlet (b)

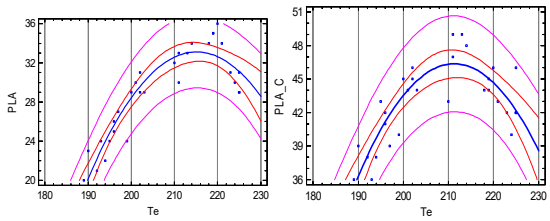

a *b*

Fige 4 Changing the calculated strength limit from PLA_C (a) and PLA (b) in a function of extruder temperature T_e

Statistical processing of the experimental results showed that the strength limit for the PLA_C material and for PLA can be satisfactorily described by polynomial equations of the second order, with a clearly defined extremum at the maximum strength point (for PLA_C $[\sigma]^{PLA\_C}$ =47,3 MPa, for PLA $[\sigma]^{PLA}$ =35,1 MPa.

The obtained indicators, in particular, HB, tensile strength along the main directions, were significantly different from those given, in particular, in [16], [19]. This effect can be explained by the fact that when calculating the critical stresses, the theoretical cross-sectional area was used, when adhesive adhesion occurred along the planes. A certain error in the established properties of the film is created by equipment and processes.

Since the field of dispersion of values for PLA_C is larger, the regression model accuracy is 71%, which can be explained by the effect of random factors caused by the presence of carbon fiber filament in the structure:

$$[\sigma]^{PLA\_C} = -944{,}076 + 9{,}37475 \cdot Te - 0{,}0221835 \cdot Te^2$$

For PLA plastic, under the condition of model adequacy of 86% and dispersion of 0.61 MPa, the corresponding regression equation will take the form

$$[\sigma]^{PLA} = -915{,}472 + 8{,}81884 \cdot Te - 0{,}0204967 \cdot Te^2$$

The laser sintering modes of the surface film were determined based on the analysis of the temperature fields created by the emitter pulse on the surface. It was not necessary to obtain penetration significant zones, we used co-focal optics with f=27 mm, the caustic tension in the focal plane was p=0.09 mm, which made it possible to determine the irradiation area s=0.00641 mm^2. We used a solid-state laser with a power of 400 W and pulse tracking frequencies ν=50; 75; 100; 150; 200 Hz, control was carried out by changing the frequency ν, Hz, the laser movement speed along the irradiated surface w, m/s, and the defocusing amount, which leads to an increase in the area of the heating spot p, mm^2. Then for the scheme of the demonstrator surface irradiation, fig. 5,a, in the form of a tube with a wall thickness of B, mm, the heat distribution will correspond to the field in Fig. 5, b, for the case of a quasi-static problem formulation. This makes it possible to predict the penetration of heat at the time of the next laser pulse arrival deep into the material and the critical temperatures appearance T_{kp} on the surface

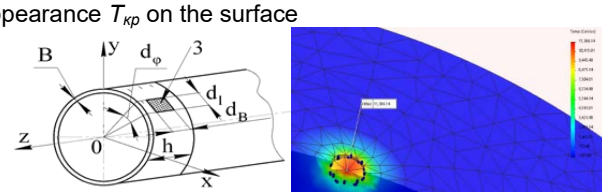

a *b*

Fig 5. Calculation scheme (a) and temperature field on the surface under the action of a single laser pulse (b).

The calculations made it possible to adopt the following film application modes: pulse tracking frequency ν=50 Hz, laser movement speed w=0.28 m/s, spot area s=0.082 mm^2 (i.e., focal length f=21.8 mm. Sintering was performed in these modes metal layer T_{kp}<290 ^{0}C.

Films obtained by Cu (Zn) deposition, fig. 6, were formed unevenly, and there were dirt particles on the surface layer, which requires more careful preparation of the components before applying the layer and improvement of the conductive sublayer before galvanization.

The sintering of Al particles turned out to be rather unsuccessful, since it was not possible to achieve structure homogeneity, fig. 6 b. The film obtained by sintering Ni powder particles showed the best result in mechanical tests, as it mechanically represented a layer of dendritic structure, fig. 7. Despite the fact that a clearly defined dendritic structure was formed during sintering, such a framework had advantages over galvanically deposited Cu (as well as Zn) particles or Al created by vacuum evaporation.

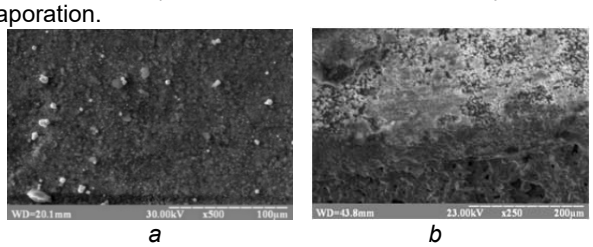

a *b*

Fig 6. Surface film formed by the galvanic method and the film layer formation during the metals vacuum deposition (in particular, Al)

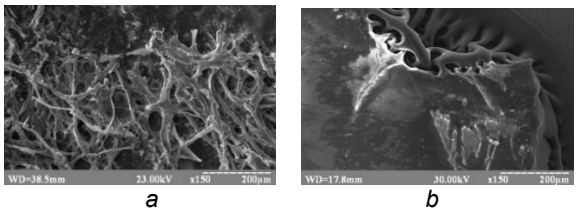

a *b*

Fig. 7 - Formation of dendritic "whiskers" from Me during surface laser scanning and formation the melt zone of a non-metallic substrate

At the same time, the formation of dendritic "whiskers" from Me during surface laser scanning was accompanied by the formation of a plastic substrate melt zone, fig. 20, b. However, no significant change in the shape or profile of the surface was created in the specified flood zones.

The specified effect was checked during the thin-walled shells production in the form of vessels that perceived working environment thermobaric loads. Vacuum ion deposition of Me was the most effective, but no performance loss of the sample was observed.

It is obvious that the main property of the film coating is to prevent the opening of microdefects at the surface and near-surface layers. Attention was also paid to the influence of the topology factors during the filament laying on the strength characteristics during tensile tests.

Testing of the deposited film without a substrate made it possible to obtain the appropriate characteristics of mechanical properties, table. 6.

Table 2. Mechanical characteristics of investigated films various types

Characteristics	Films and surface layers		
	Chemical	Physico-chemical	Thermo-mechanical
	Glues	Galvanic	Laser sintering
Thickness, mm	0,2…0,5	30…60	25…80
Adhesion, MPa	35…40	28…30	27…30
Hardness, HB	-	55	<110
Tensile strength, MPa	12…15	<30	70
Hollowness, %	-	0,5	2…3

Considering the obtained results, the next investigations should be conducted for assessing the possibility of providing geometric parameters and implementing the process of applying the film was to manufacture the demonstrators (honeycomb tank, for example)

A comparison of the patterns of reinforced plastics destruction and ordinary ones proved that the obtained data have a significant difference in the plane of filament laying on the "blade" type samples, but they differ little for the layers located perpendicular to the direction of the force and can practically be attributed to one general population when studying the samples on stretching. Applying a film on the surface of the demonstrators and samples proves that the destruction changes pattern, and instead of the development of a defects significant number with the formation a collection of destruction places, a well-defined critical intersection zone is formed, which coincides with the simulated state, and in which the development of defects leads to complete destruction sample.

Conclusions

The technological bases of the formation of complex profile products using the 3-D FDM process and the films application allow to significantly increase the resistance to the shells destruction. The shells strength reaches 90% of the filament strength. This approach changes the paradigm of the additive technologies applications, allowing the creation of low-strength hollow shells that are suitable for the deposition of surface films by "cold" and "hot" methods.

At the same time: strength indicators, especially for thin-walled shells, are not satisfactory; even despite the establishment of rational conditions for laying out the filament, as well as the involvement of improving the adhesive contact technical means, the permissible strength indicators $[\sigma_u]=0,75…0,8[\sigma_т]$, $[\sigma_т]$, - the strength limit of the filament material, were obtained.

The application of surface films even 0.3 mm thick significantly increases the tested samples strength, while changing the mechanism of destruction: the avalanche-like development of initial defects set ceases to be observed, and critical intersection zones are formed, which are satisfactorily predicted by existing computer systems. Strength increases to [u]=0,95…0,98[t].

***Authors**: Mykhaylo Zagirnyak, Rector, Kremenchuk Mykhailo Ostrohradskyi National University, Professor, 20, Pershotravneva street, Kremenchuk, 39600, Ukraine, E-mail: mzagirn@gmail.com*
Oleksandr Salenko, Professor of the Department of Machine Design, Sikorskyi NTUU KPI, Kyiv, Ukraine, E-mail: salenko2006@gmail.com
Walid Alnusirat, Associate professor at Al-Balqa Applied University, E-mail: alnusirat_w@protonmail.com
Leonid Golovko, Department of Laser Systems and Advanced Technologies Sikorskyi NTUU KPI, Kyiv, Ukraine
Vadym Orel, Department of scientific work organization and gender issues, Kremenchuk flight college Kharkiv National University of Internal Affairs Kremenchuk, Ukraine, E-mail: deoxis24@gmail.com
Viktoriia Kulynych, Department of Manufacturing Engineering Kremenchuk Mykhailo Ostrohradskyi National University Kremenchuk, Ukraine, E-mail: vikulsija@gmail.com

REFERENCES

[1] E. Canessa, C. Fonda, M. Zennaro, Low-cost 3D Printing for Science, Education & Sustainable Development, 1st ed., ICTP-The Abdus Salam International Centre for Theoretical Physics, Trieste, Italy, 2013.
[2] J. T. Quigley, Chinese Scientists Are 3D-Printing Ears and Livers – With Living Tissue, 2013. URL: https://thediplomat.com/2013/08/chinese-scientists-are-3d-printing-ears-and-livers-with-living-tissue/
[3] ABS and PLA plastics. What is the difference between ABS plastic and PLA plastic. URL: http://picaso-3d.com/ru/abs-i-pla-plastiki/
[4] V. V. Pushkarev, A. V. Drobotov, Arrangement of devices for volume printing by extruded molten parts of complex shape, in: Proceedings of Volgograd State Technical University, 20 (2013), 121-123.
[5] Park J, Tari MJ, Hahn HT. Characterization of the laminated object manufacturing (LOM) process. Rapid Prototyp J 2000;6(1):36–50.
[6] Liao Y, Li H, Chiu Y. Study of laminated object manufacturing with separately applied heating and pressing. Int J Adv Manuf Technol 2006;27(7–8):703–7.
[7] Liao Y, Chiu Y. Adaptive crosshatch approach for the laminated object manufacturing (LOM) process. Int J Prod Res 2001;39(15):3479–90.
[8] L. Momoda. “The future of engineering materials: Multifunction for performance-tailored structures”. Bridge, vol. 34 (2004): 18–21.
[9] L. Puig, A. Barton, and N. Rando. A review on large deployable structures for astrophysics missions. Acta Astronautica, vol. 67, no. 1-2, (2010): 12–26.
[10] Doely, P.K. 3D Printing: A New Dimension in Construction. http://fwhtlaw.com/briefing-papers/3d-printing- new-dimension-construction. Accessed 9 February 2022.
[11] Xu Sheng-jin, Kong Xian-ren, Wang Ben-li, MA Xing-rui, Zhang Xiao- chao. Method of equivalent analysis for statistics and dynamics behavior of orthotropic honeycomb sandwich plates, Acta Materiae Compositae Sinica. 17(3) (2000): 92-95.
[12] Salenko, A., Melnychuk, P., Lashko, E., Derevianko, I., Samusenko, O.: Ensuring The Functional Properties of Responsible Structural Plastic Elements by Means of 3-D Printing. Eastern-European Journal of Enterprise Technologiesthis link is disabled. 5(1-107), 18-28, (2020).
[13] Meifeng He, Wenbin Hu, A study on composite honeycomb sandwich panel structure, Materials and Design, 29 (2008) 709–713.
[14] Comparizen mechanical propertiez of ABS and PLA filaments https://www.liqcreate.com/supportarticles/properties-fdm-sls-resin/. Accessed 9 February 2022.
[15] Özalp, F., Yilmaz, H.D.: Fresh and Hardened Properties of 3D High-Strength Printing Concrete and Its Recent Applications. Iran. J. Sci. Technol.-Trans. Civ. Eng. 44, 319–330, (2020).
[16] Guoxin Fang, Sikai Zhong, Zichun Zhong, Tianyu Zhang, Xiangjia Chen, Charlie C L Wang: Reinforced FDM: Multi-Axis Filament Alignment with Controlled Anisotropic Strength. ACM Transactions on Graphics. 39, 6 (2020). doi: 10.1145/3414685.3417834.
[17] Mohammed A. Isa, Ismail Lazoglu: Five-axis additive manufacturing of freeform models through buildup of transition layers. Journal of Manufacturing Systems 50, December 2018, 69–80, (2019). doi:10.1016/j.jmsy.2018.12. 002.
[18] Gardner, J.A., Kaill, N., Campbell, R.I., Bingham, G.A., Engstrøm, D.S., Balc, N.O.: Aligning Material Extrusion Direction with Mechanical Stress via 5-Axis Tool Paths. In 29th Annual International Solid Freeform Fabrication Symposium. An Additive Manufacturing Conference, SFF. 2005–2019, (2018).
[19] W. Alnusirat, A. Salenko, S. Shlyk, I. Gusarova, P. Loboda, I. Trosnikova, and I. Bogomol, Ensuring Strength of the Seam of Thermal Protective Structures from Thin-Sheet Nickel Alloys Obtained by Laser Vacuum Welding, Metallofiz. Noveishie Tekhnol., 44, No. 3 (2022): 393–418 doi: 10.15407/mfint.44.03.0393